



Numerical analysis of ground improvement effects on dynamic settlement of uniform sand using DEM

Hadi Ahmadi¹ · Saman Farzi Sizkow²Received: 28 October 2019 / Accepted: 12 March 2020 / Published online: 18 March 2020
© Springer Nature Switzerland AG 2020

Abstract

Uniform fine sands are recognized as problematic soils which are highly prone to earthquake or dynamic loads effects. Cyclic and dynamic loads on such soils can destroy its structure and cause them to experience high volume change. In loose sands, volume change originated from dynamic or cyclic loadings (caused by earthquake, machineries or other similar sources) can lead to excessive settlements on the ground surface which in turn endangers the structural integrity and performance of the superstructure. As a consequence, it is important to perform soil improvements prior to putting any foundation on them. Among many known and recently developed techniques, the soil compaction (or densification) and cement injection are the widest techniques in fine sands improvement. In this research, a numerical study is employed which incorporates the distinct elements method to investigate the volume change and settlement of uniform fine sands. The results obtained numerically have been compared with those observed in a laminar shear box physical model of samples of fine sand. A surface footing is placed over the top of the specimen in the shear box which is modeled by a small rigid plate. Comparisons indicate that the applied simulation technique is suitable for the soil under study. To simulate the model and for verification purpose, Anzali sand physical and mechanical properties have been implemented. Soil particles in the discrete elements technique were modeled by spherical particles obeying the Anzali sand grain size distribution, and for the surface footing, rigid clumps of particles were used. Experiments were performed for density indices of 30–88%, and numerical simulations by the discrete elements method were performed at porosities of 0.43–0.38. The trend of dynamic settlement over the cyclic loading shows a good agreement with measured data in the laboratory. Results revealed that the improvement techniques such as compaction and cementation have a significant effect on the reduction in the final settlement under applied dynamic loads.

Keywords Dynamic settlement · Distinct element method · Cyclic loading · Anzali sand · Cementation

1 Introduction

Recent extensive studies demonstrate that cyclic and dynamic loadings produced by earthquake, urban trains and machineries, especially when acting in horizontal direction, can induce large settlements in sands. These dynamic settlements are more severe in loose sands and may exceed the allowable limit. During cyclic loading phase, a soil sample may become dense or loose as

cumulative shear deformations develop in it. The cumulative volumetric changes and shear deformation behavior of a soil sample depend largely on static stress conditions before applying the load. According to conservation of energy principle, the work done on a soil sample during cyclic loading phase dissipates through rearrangement of soil particles which causes irreversible strains in the soil. Silver and Seed (1971) propose a method for estimating settlement of the unsaturated sand during earthquake

✉ Hadi Ahmadi, hadiahmadi@guilan.ac.ir | ¹Department of Civil Engineering, University of Guilan, Rasht, Iran. ²School of Civil and Environmental Engineering, Southern Methodist University, Dallas, TX, USA.



[1]. The effects of dynamic loads on compaction and subsequent settlement of granular soils (non-cohesive soils) have always been a subject of interest for many researchers [2]. Analyzing the performance of 32 improved sites in the USA and Japan after Northridge (1994) and Kobe (1995) earthquakes shows that the settlement, lateral spreading, instability and liquefiability of improved sites subjected to seismic shaking are significantly lower than adjacent intact sites. The difference between amounts of dynamic settlement in these sites is higher than 50 cm in some cases [4]. Furthermore, after 1970s, the effect of cementation on behavior and strength characteristics of coarse sands became a serious topic and a number of papers were published in this area. These experiments are mostly conducted using sandy soil and synthetic cement (a combination of Portland cement, lime, plaster, baked clay and other chemicals). Investigation of cementation effects on strength and deformability of sand by Vinoth et al. [5] is an example of these studies. Ahmadi et al. have studied the effect of three different soil stabilization techniques including densification, draining and cementation using experimental tests and have shown that the cementation method is an admirable technique on the mitigation of dynamic settlement [6]. Since in situ measuring, field studies and realistic modeling are time-consuming, expensive and require special equipment, numerical modeling and computer-aided simulation have been increasingly used in recent years to predict the behavior of soil.

In this study, the effects of ground improvement methods (compaction and cementation) on the dynamic settlement of clean sands under cyclic loading are investigated through numerical simulation and physical modeling. Numerical simulations are performed using distinct element method, and physical modeling is done with the aid of laminar box apparatus.

2 Physical modeling

2.1 Laboratory apparatus

In order to study the dynamic settlement of uniform fine-grained sands, small-scale physical modeling is performed by a series of laboratory tests on the samples. A laminar box placed on a shaking table is employed for this purpose. The laminar box has dimensions of 600 mm in lateral directions and 580 mm in vertical direction. The laminae, external protective case and box floor are made of transparent Plexiglas so that inside of the box is visible from all angles. The flexible wall is composed of eight laminae with thicknesses of 50 mm. Horizontal cyclic movement of the laminar box is driven by an electromotor and can have frequencies of up to 4 Hz and the

maximum amplitude of 15 mm. A rigid metal plate with dimensions of 100 mm × 100 mm × 50 mm represents the foundation system, and a hydraulic jack applies the target pressure on the sample. The roller bearings installed at the end of hydraulic jack shaft allow horizontal displacement of loading plate to minimize the shear stresses under the footing. The hydraulic jack plate exerts a constant pressure on the sample, and as the sample surface level changes, the hydraulic jack shaft displaces vertically to keep the pressure at a steady level. Regarding the connection type between the hydraulic jack shaft and loading plate, the foundation can freely change in area and thickness. Figure 1 shows a picture of the laminar box apparatus. The geometrical details and components of the laminar box are shown in Fig. 2. Further information is provided by Ahmadi et al. [7].

2.2 Anzali sand

Samples of Anzali sand are chosen for the physical model tests and calibration of numerical models. Most of the sandy soils found in Anzali are composed of uniformly graded loose-to-medium sands with fine-to-very fine grain size. Geotechnical investigations performed at various sites in this area confirm this fact [8]. The SPT numbers for subterranean layers obtained from geotechnical investigations are generally between 10 and 30 blows; therefore, these layers have low-to-medium densities. The most common constituent of Anzali sand is silica. It has a D_{50} value between 0.2 and 0.3 mm and is regarded as poorly graded sand with a narrow particle size range. Studies on shear strength parameters of Anzali sand suggest that, for a sample of clean sand under consolidation stress of 150 kPa, the corresponding friction angle is approximately 30 degrees and a 20% increase in number of silty grains reduces the friction angle to 26 degrees. The particle size distribution



Fig. 1 Picture of the laminar box apparatus

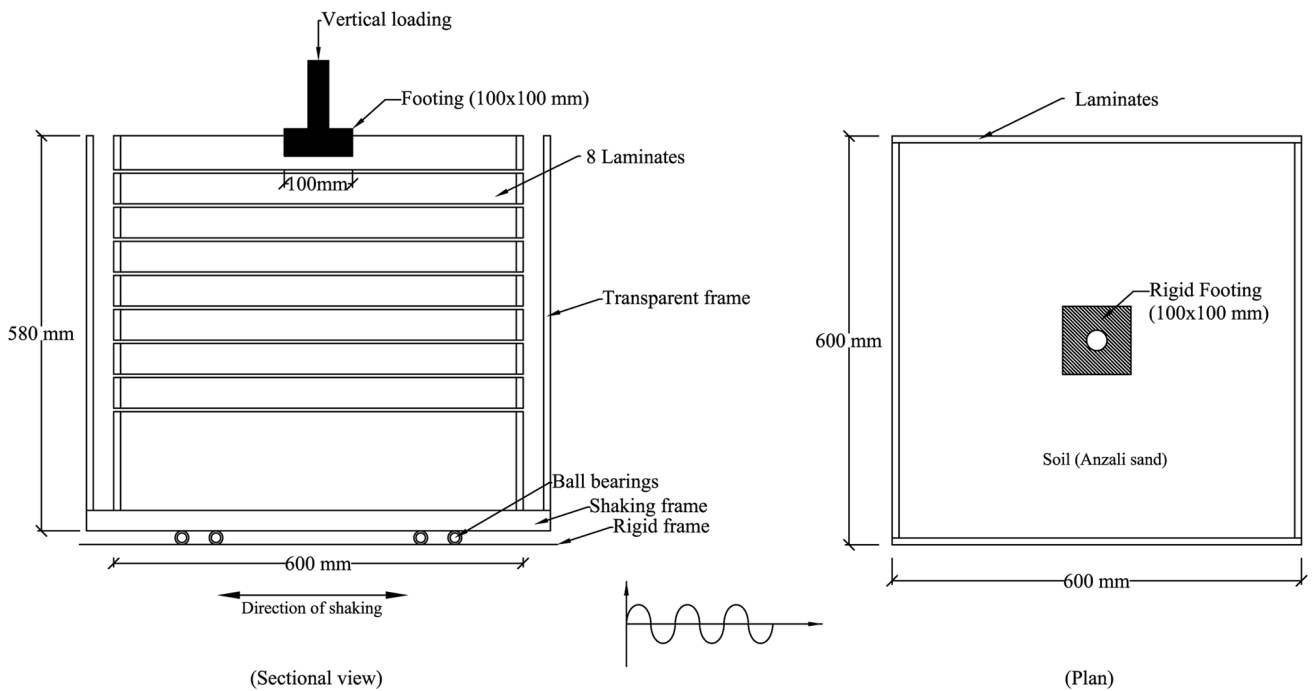


Fig. 2 Geometrical details and components of the laminar box [5]

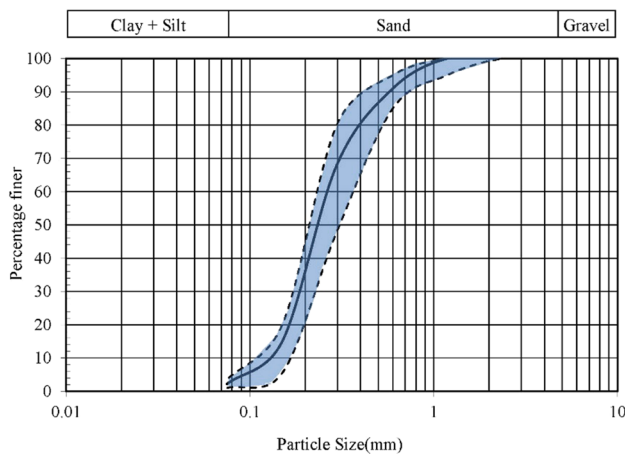


Fig. 3 Grain size distribution of the samples

of Anzali sand is shown in Fig. 3, and its properties are listed in Table 1.

2.3 Sample preparation and testing condition

Three dry samples of Anzali sand with relative densities of 30, 50 and 80% are created which represent the loose, medium and dense states, respectively. The samples are subjected to a cyclic excitation produced by the shaking table with frequency of 2 Hz and maximum acceleration amplitude of 0.24 g, and the footing pressure is set to 30 kPa. Figure 4 shows the seismic acceleration applied

Table 1 Properties of Anzali sand

Parameter	Value
Classification	SP
Coefficient of uniformity (Cu)	2.28
Coefficient of curvature (Cc)	1.11
Specific gravity (Gs)	2.66
Maximum void ratio (emax)	0.83
Minimum void ratio (emin)	0.57
Average grain size (D_{50})	0.24 mm
Effective grain size (D_{10})	0.12 mm

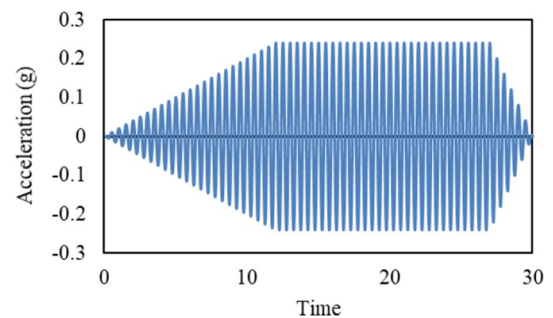


Fig. 4 Base cyclic acceleration

by the shaking table. Since the data recording is done after the static settlement of the specimen is occurred, the vertical displacements of footing plate achieved from

this experiment only denote the dynamic settlement. The cyclic loading continues for 30 s, and the experimental data are gathered for 60 s. The ground improvement process is done by injection of cement into the samples. Four injecting pipes with diameter of 3.4 inch (approximately 19 mm) and length of 500 mm are driven into the samples at four sides of the square footing, and distance between the center of pipes and square footing edge is about 100 mm. Every pipe has 24 holes with diameters of 4 mm and 50 mm gaps between them. The water-to-cement ratio is set to one, and the cement slurry is blended by a mixer for 30 s. The samples are loaded after 28 days.

2.4 Laboratory results

Figure 5 illustrates the dynamic settlements of samples of Anzali sand recorded during laminar box test. S/B is the dynamic settlement-to-footing width ratio. It can be observed from Fig. 6 that the dynamic settlement increases almost linearly (especially for loose sample) with

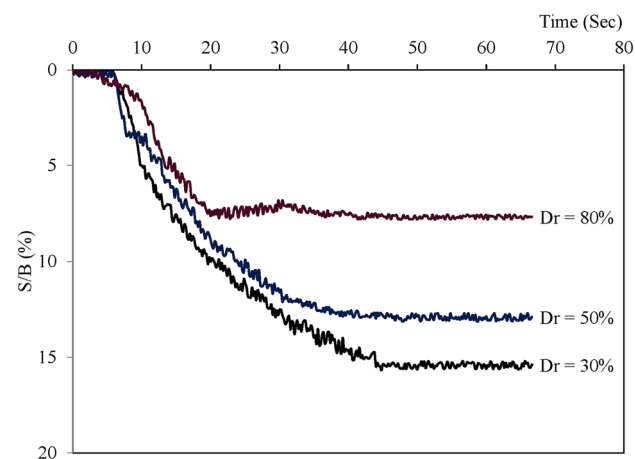


Fig. 5 Laboratory results of dynamic settlement ratios for samples with different porosities

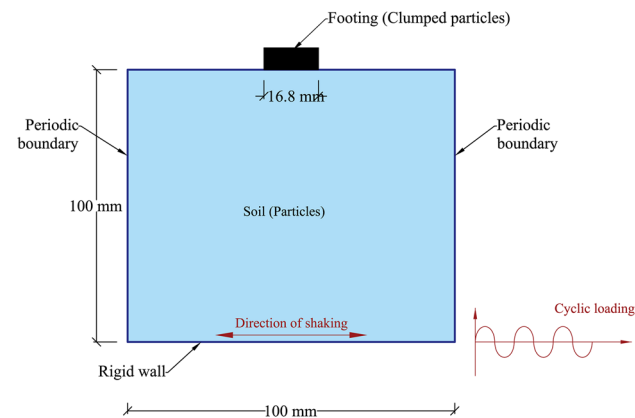


Fig. 6 Schematic configuration of DEM model

the number of loading cycles. The loose sample settlement continues even after the cyclic loading period is ended. In addition, sudden changes in the surface level of loose sample are observed. After approximately 22 s, the relative density of dense sample increases from 88 to 98% and the foundation experiences a gradual uplift which is caused by dilation of uniform sand. This uplift is more obvious in the surface of sample surrounding the footing. The results reveal that S/B value varies from 3.8% for loose sample (relative density of 30%) to 1.5% for dense sample (relative density of 88%) which indicates a 55% drop in settlement amount. Literature review shows that the laboratory results presented in this study are in a good accordance with the data provided by Coelho et al. and Ueng et al. for similar conditions [9, 10]. It is worth mentioning that in this condition, shear stiffness and subsequent elastic modulus of sample increase and a considerable decrease in static settlement is expected as well.

3 Numerical modeling

3.1 Distinct element method

Distinct element method is a powerful numerical technique mainly developed for modeling of discontinuous systems consisting of particles. DEM simulation systems have four principal components: object representation, contact detection, physics and visualization [11]. In contrary to finite element and finite volume methods, distinct element method is a mesh-free method. A DEM model is composed of a number of distinct rigid particles representing soil grains which can move independently and are allowed to overlap one another at contact points. A DEM calculation cycle involves repeated application of Newton's second law of motion and the force-displacement law in order to compute the forces and motions inside an assembly of particles. Newton's second law of motion is applied to each particle to calculate its motion which is resulted from the contact and body forces, and the force-displacement law is applied to each contact to determine the contact forces created by relative motions of particles at each contact point. Therefore, in this manner, particle movements and contact forces at any point of the system can be traced.

Distinct element method was originally proposed by Candull [12] to simulate the mechanical behavior of jointed rocks and was later developed by Candull and Stark [13] to BALL program for modeling granular media by two-dimensional disks. Today, the application of distinct element method in simulation of micromechanical behavior of granular soils is rapidly spreading. Substantial progress is made in DEM modeling of laboratory tests

such as direct shear test [14], triaxial test [15], true triaxial test [16], cyclic triaxial test [17], cyclic loading [18], hollow cylinder torsional test [19] and oedometer consolidation test [20]. Elshamy and Zamani employed distinct element method to analyze the seismic response of shallow foundations considering soil–foundation–structure interactions. In the mentioned study, a single-degree-of-freedom structure is founded on a dry granular soil deposit by a rigid square spread footing [21]. de Bono et al. studied the effect of cementation on the degree of crushing using the discrete element method. It was shown that in the cemented material, an increase in the degree of crushing was observed with increasing cement content [22]. Shen et al. were developed a three-dimensional bonded contact model to simulate the mechanical behavior of bonded granular material using the DEM. The parametric studies were shown that three parameters, including the bond material properties, the bond content and the bond distribution have the most influence on the behavior of cemented sand [23].

3.2 The DEM model

In this study, PFC^{3D} (Particle Flow Code in Three Dimensions) is used for DEM simulation of the mechanical behavior of physical models [24]. Due to computational limitations, the high g-level concept and scaling laws for dynamic centrifuge test are employed to decrease the domain size. In addition, particle sizes are enlarged to reduce the number of particles and consequently shorten the simulation length. However, as is described later in this section, micro-properties are adjusted in a way that bulk properties of numerical model match those of physical model. Due to the increase in grain size, the scale of the other parameters is calculated based on the results of lai et al. [25]. Accordingly, the scaling factor (prototype/virtual model) for strain (μ_ϵ) is computed by

$$\mu_\epsilon = \mu \left(\frac{(V_s)_m}{(V_s)_p} \right)^2 \quad (1)$$

where μ is the scaling factor for length, $(V_s)_m$ is the shear wave velocity of soil deposits in the model, and $(V_s)_p$ is the shear wave velocity of soil deposits in the prototype, as recommended by lai et al. (2005) for model tests on loose sands ($\mu_\epsilon = 1$). Thus, the scaling factor of length (μ), density (μ_ρ) and strain (μ_ϵ) is equal to 1/6, 1 and 1, respectively. By applying these factors, the values used in the input parameters are given in Table 2. The DEM model dimensions are 100 mm (600 mm for the physical model) in lateral directions and 83.3 mm (500 mm for the physical model) in vertical direction. An assembly of particles with

Table 2 Input parameters for DEM simulation

Parameter	Value
<i>Assembly of particles</i>	
Diameter	4 to 6 mm
Normal stiffness	5×10^5 N/m
Shear stiffness	5×10^5 N/m
Normal critical damping ratio	0.1
Shear critical damping ratio	0.0
Friction coefficient	0.5
Density	2660 kg/cm ³
Porosity	0.38 to 0.43
<i>Boundary conditions (walls)</i>	
Normal stiffness	10^8 N/m
Shear stiffness	10^8 N/m
Friction coefficient	0.5
<i>Parallel bonds</i>	
Normal stiffness	5.1×10^{10} N/m ²
Shear stiffness	5.1×10^{10} N/m ²
Normal strength	1.5 MPa
Shear strength	1.5 MPa
Radius multiplier	0.5
<i>Computation parameters</i>	
g-level	6.0
Maximum cyclic acceleration	1.44 g
Time step	3.5×10^{-6} s

a size range of 4–6 mm is generated inside the domain and is subjected to a high gravitational field of 6 g to satisfy the scaling laws. The periodic boundaries are specified at the lateral sides to avoid the reflection of propagating waves. This type of boundary simulates a condition in which the model is endlessly repeated in each lateral direction. When a particle exits through one side of the domain, an identical particle with the same velocity enters from the opposite side. The loading platen is modeled by a rigid raft made of clumped particles with lateral dimensions of 16.66 mm (100 mm for physical model). Figure 6 shows the schematic configuration of numerical system. Vertical forces are applied to the clumped particles to provide the required pressure. A rigid wall at the bottom of the model represents the shaking table. A cyclic acceleration with maximum amplitude of 1.44 g (0.24 g for the physical model) is applied to the base wall for 5 s (30 s for the physical model) to comply with scaling laws. The DEM model is demonstrated in Fig. 7.

In order to choose the most realistic values for micro-properties, since they cannot be directly extracted from the physical sample, a series of triaxial tests are numerically conducted using PFC^{3D} and parameters are varied until the macro-properties of numerical model match

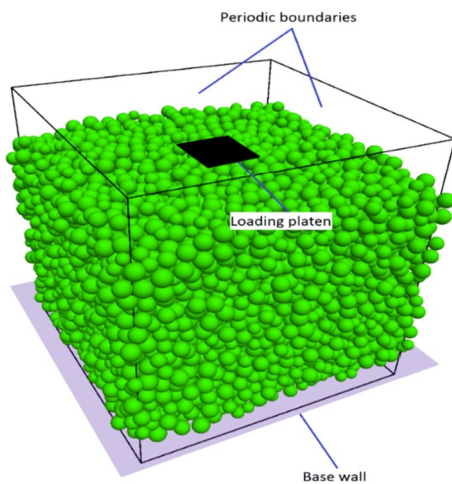


Fig. 7 DEM model

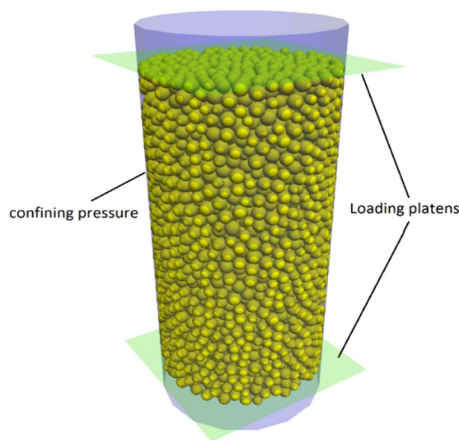


Fig. 8 DEM model for simulated triaxial test

known properties of physical sample. The main guidelines to choose particle properties more efficiently are:

- The Young’s modulus of the assembly is linearly related to the values of particle stiffness
- The peak strength of the assembly, in the absence of parallel bonds, mainly depends on the friction coefficient

Figure 8 illustrates the numerical model used in the simulated triaxial test. A cylindrical wall with diameter of 7.5 cm and height of 15 cm provides a confinement pressure of 150 kPa. The deviatoric stress is produced by two planar walls at the top and bottom of the model. Plots of axial deviatoric stress and volumetric strain versus axial strain, for the case that particle stiffness and friction coefficient are set to 5×10^5 N/m and 0.5, are given in Fig. 9 and Fig. 10, respectively. In this case, Young’s modulus and friction angle

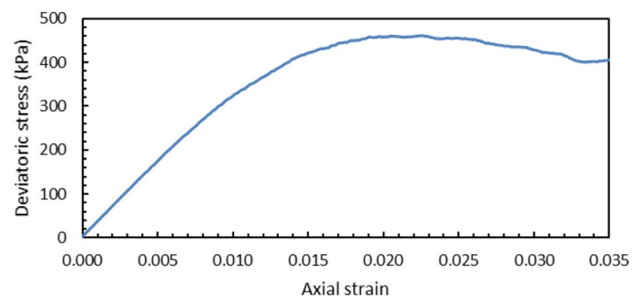


Fig. 9 Deviatoric stress versus axial strain

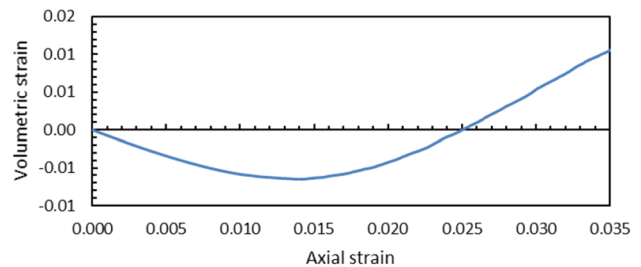


Fig. 10 Volumetric strain versus axial strain

derived from the simulated triaxial test are similar to physical model. Therefore, these values are used in simulation of the laminar box test.

PFC^{3D} provides contact and parallel bonds to simulate cohesive and cemented soils, respectively. To model the cementation process, parallel bonds are installed at contact points. The parallel bonds act as a set of elastic springs working in parallel with point-contact springs that are used to model particle stiffnesses. Relative displacements of two bonded particles induce a force and a moment within the bond material which are related to maximum normal and shear stresses within the bond material. Parallel bond breakage happens when one of these stresses exceeds the corresponding bond strength. A list of parameter used in the laminar box simulation is provided in Table 2.

4 Results and Discussion

The main focus of DEM analysis is on the dynamic settlements occurred under the loading plate. The simulation is performed for assemblies of particles with different porosities. The relative density (D_r) can be calculated by:

$$D_r = \frac{e_{\max} - \frac{n}{1-n}}{e_{\max} - e_{\min}} \tag{2}$$

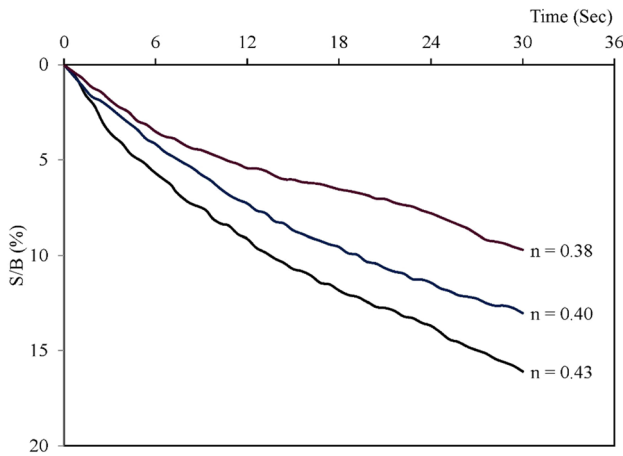


Fig. 11 DEM simulation results for dynamic settlement-to-footing width ratios of assemblies with different porosities

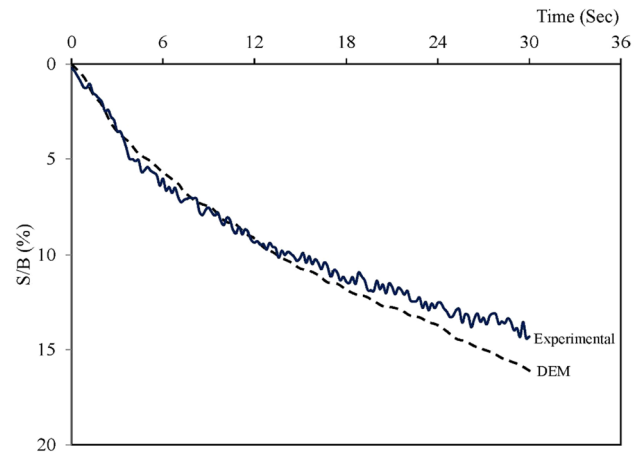


Fig. 13 Comparison between dynamic settlements of loose sample obtained from DEM simulations and laboratory tests

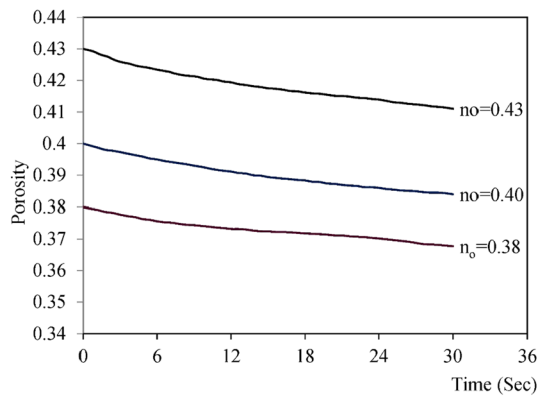


Fig. 12 DEM results for porosities of samples versus time

where n is the porosity of sample and e_{max} and e_{min} are the maximum and minimum void ratios. According to the results of laboratory tests (Table 1), the samples with relative densities of 29.1 and 83.5% have porosities of 0.43 and 0.38 which signify loose and dense states, respectively. Figure 11 demonstrates the dynamic settlement of samples caused by the application of cyclic load. To neutralize the scaling effect, results are presented as settlement-to-footing width ratio (S/B). It can be seen from Fig. 11 that as simulation continues, the dynamic settlement increases with a relatively steady rate (especially in loose sample). However, the settlement curve has a milder slope for the dense sample. The porosities of samples as functions of time are plotted in Fig. 12. It is apparent from Fig. 12 that the porosity of loose sample drops with a higher rate, while the porosity of dense sample becomes almost constant after a few seconds.

Figure 13 shows a comparison between the dynamic settlements induced by cyclic loading in the loose sample

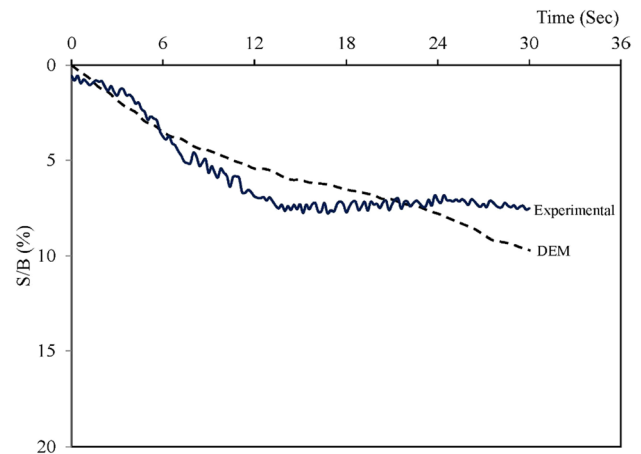


Fig. 14 Comparison between dynamic settlements of dense sample obtained from DEM simulations and laboratory tests

obtained from DEM simulation and physical modeling. The physical sample has relative density of 30%, and the DEM assembly of particles has a porosity of 0.43. It can be seen that DEM data are compatible with the laboratory results. Comparison between results of numerical simulations and laboratory tests for the dense sample is shown in Fig. 14. The dense sample has relative density of 88%, and an assembly of particles with porosity of 0.38 serves for this purpose in DEM simulations. Although the ultimate dynamic settlement values reported by these two methods are relatively close, the settlement amount changes with a steadier rate for DEM simulation. Since the sand grains are simplified as spherical particles in DEM models, the ultimate dynamic settlement predicted by numerical simulation is slightly higher than laboratory results and the sample dilation is not noticeable in DEM simulation. Grain interlock has a significant effect on deformability

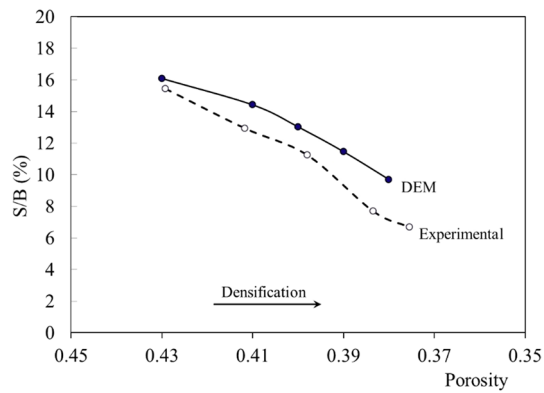


Fig. 15 DEM simulation and laboratory results for final dynamic settlements of samples versus porosity

of the sample and can considerably change the amount of settlement. The comparison of numerical and experimental data for final dynamic settlement of samples with different porosities is shown in Fig. 15. The maximum and minimum discrepancies between results are 4 and 26%. The gap between the results is larger for the dense sample. This can be attributed to the fact that, in experimental tests, the grains are not completely similar or identical in shape and angularity. Therefore, in dense conditions, the interlock and contact surface is more exposed. Therefore, the compressibility is reduced and the difference with the numerical results is increased. Numerical simulation predicts volumetric strains of 3.22 and 1.87% for loose and dense states, respectively. This means that the dynamic settlement of sand is reduced by 42% (compared to 55% obtained from laboratory results) through compaction. Numerical simulation based on macro-properties of physical samples is conducted using distinct element method, and there is consistency between results of physical modeling and numerical simulation. In order to reduce the simulation length, the scaling laws for dynamic centrifuge test are applied to input parameters and output data of DEM simulations. The result shows that the DEM simulation can predict the dynamic settlement of sands with a good accuracy.

The dynamic settlement of loose sample after installation of parallel bonds is shown in Fig. 16. The results reveal that since cementation creates a paste between the sand layers, it can dramatically reduce the amount of dynamic settlement. Therefore, the damages caused by earthquake can be minimized and the uneven settlements of foundation will be eliminated. The effect of cementation on the reduction in sand settlement is due to intergranular adhesion. In the distinct element method, this resistive force is provided by the bonding network on the contact forces. In cemented sand, the bonding network remains intact at small strains. Therefore, many particles

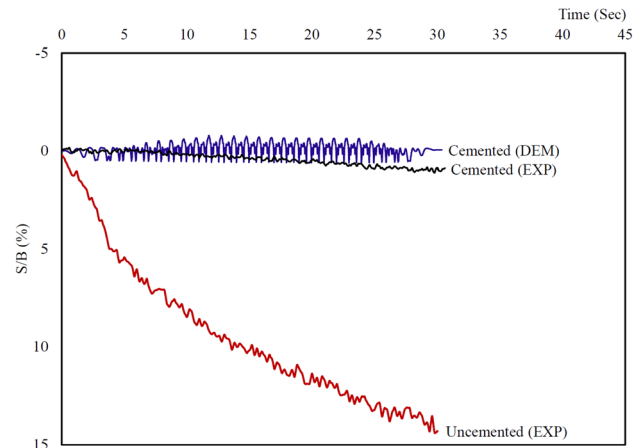


Fig. 16 DEM simulation and laboratory results for dynamic settlement of cemented loose sand

will be able to contribute to the force-chain distribution. For the unbonded particles, the maximum shear force at contacts can be obtained from the internal friction, while the bonding network assumes the presence of real cohesion between sand particles at the cemented sand, and it mitigated the strains in comparison with the case of uncemented particles.

5 Conclusion

The study of dynamic settlement is an essential part of geotechnical design process for structures built on uniform sandy soil. Soil compaction is an effective tool for controlling and reducing this type of settlement. The laboratory tests performed using laminar box apparatus on three samples of Anzali sand with different relative densities show that soil compaction can significantly reduce the ultimate dynamic settlement of granular soils and increasing the relative density from 30 to 88% causes a 55% decrease in the ultimate dynamic settlement of sample. Although comparing numerical modeling with the distinct element method for estimating dynamic settlement of sands, with experimental results in similar conditions, showed a difference of 4–26%, the process of estimating dynamic settlement is desirable. This comparison shows that this method is a very effective tool for estimating the dynamic settlement of granular soils. Both experimental and numerical results have shown that the densification technique is a suitable method for reducing settlement under dynamic loading. In addition, the simulation results support the fact that cementation can minimize the ultimate dynamic settlement and eliminate the consequent damages caused by earthquake.

Compliance with Ethical Standards

Conflict of interest Furthermore, there are no conflicts of research to be reported.

Human and animal rights No human/animal rights issue is relevant herewith.

References

- Silver ML, Seed HB (1971) Volume changes in sands during cyclic loading. *J Soil Mech Found Div ASCE* 97:1171–1182
- Ahmadi H, Eslami A, Arabani M (2017) Experimental study on the settlement of marine deposits of Anzali under cyclic loading by laminar box apparatus. *Mar Georesour Geotechnol* 35(3):330–338. <https://doi.org/10.1080/1064119X.2016.1164771>
- Eslami A (2004) Foundation engineering design and construction. BHRC Publication, Tehran, pp 104–124
- Eslami A (1999) Performance of stabilized ground during and after earthquake. In: Proceeding of the 6th annual symposium of analytical and experimental investigation of structures subjected to earthquake and dynamic loading, Rasht, Iran, pp 92–121
- Vinoth G, Moon SW, Moon J, Ku T (2018) Early strength development in cement-treated sand using low-carbon rapid-hardening cements. *Soils Found* 58(5):1. <https://doi.org/10.1016/j.sandf.2018.07.001>
- Ahmadi H, Eslami A, Arabani M (2017) Mitigating the seismic settlement of foundations on sand by ground improvement techniques. *Proc Inst Civ Eng Ground Improv* 170(2):72–80. <https://doi.org/10.1680/jgrim.15.00035>
- Ahmadi H, Eslami A, Arabani M (2015) Laminar box apparatus of the University of Guilan: commissioning. In: 2nd International conference on Geotechnical and Urban earthquake engineering, Tabriz, Iran
- Ahmadi H (2016) Settlement of sand under monotonic and cyclic loading considering soil improvement; case study: Anzali Sand. PhD thesis, University of Guilan, Iran, p 225
- Coelho PA, Haigh SK, Madabhushi SPG (2004) Centrifuge modeling of liquefaction of saturated sand under cyclic loading. In: Proceedings of the international conference on cyclic behaviour of soils and liquefaction phenomena. Taylor & Francis Group, pp 349–354
- Ueng TS, Wu CW, Cheng HW, Chen CH (2012) Settlements of saturated clean sand deposits in shaking table tests. *Soil Dyn Earthq Eng* 30(1–2):50–60. <https://doi.org/10.1016/j.soildyn.2009.09.006>
- O'Connor RM, Torczynski JR, Preece DS, Klosek JT, Williams JR (1997) Discrete element modeling of sand production. *Int J Rock Mech Min Sci* 34:3–4. [https://doi.org/10.1016/S1365-1609\(97\)00198-6](https://doi.org/10.1016/S1365-1609(97)00198-6)
- Cundall PA (1971) A computer model for simulating progressive, large-scale movements in blocky rock systems. In: Proceedings of the symposium on Znt. Sot. Rock Mech., Nancy 2, NO. 8
- Cundall PA, Strack ODL (1979) A discrete numerical model for granular assemblies. *Geotechnique* 29(1):47–65. <https://doi.org/10.1680/geot.1979.29.1.47>
- Wang J, Gutierrez M (2010) Discrete element simulations of direct shear specimen scale effects. *Geotechnique* 60(5):395–409. <https://doi.org/10.1680/geot.2010.60.5.395>
- Binesh SM, Eslami-Feizabad E, Rahmani R (2018) Discrete element modeling of drained triaxial test: flexible and rigid lateral boundaries. *Int J Civ Eng* 16(10):1463–1474. <https://doi.org/10.1007/s40999-018-0293-0>
- Torres SAG, Pedroso DM, Williams DJ, Mühlhaus HB (2013) Strength of non-spherical particles with anisotropic geometries under triaxial and shearing loading configurations. *Granul Matter* 15:531–542. <https://doi.org/10.1007/s10035-013-0428-6>
- Nguyen NS, François S, Degrande G (2014) Discrete modeling of strain accumulation in granular soils under low amplitude cyclic loading. *Comput Geotech* 62:232–243. <https://doi.org/10.1016/j.compgeo.2014.07.015>
- Hu M, O'Sullivan C, Jardine RR, Jiang M (2010) Stress-induced anisotropy in sand under cyclic loading. *Granul Matter* 12:469–476. <https://doi.org/10.1007/s10035-010-0206-7>
- Ravichandran N, Machmer B, Krishnapillai H, Meguro K (2010) Micro-scale modeling of saturated sandy soil behavior subjected to cyclic loading. *Soil Dyn Earthq Eng* 30:1212–1225. <https://doi.org/10.1016/j.soildyn.2010.05.002>
- de Bono J, McDowell G (2015) An insight into the yielding and normal compression of sand with irregularly-shaped particles using DEM. *Powder Technol* 271:270–277. <https://doi.org/10.1016/j.powtec.2014.11.013>
- El Shamy U, Zamani N (2011) Discrete element method simulations of the seismic response of shallow foundations including soil- foundation- structure interaction. *Int J Numer Anal Meth Geomech* 36(10):1303–1329. <https://doi.org/10.1002/nag.1054>
- Bono JP, McDowell GR, Wanatowski D (2014) DEM of triaxial tests on crushable cemented sand. *Granular Matter* 16(4):563–572. <https://doi.org/10.1007/s10035-014-0502-8>
- Shen Z, Jiang M, Thornton C (2016) DEM simulation of bonded granular material. Part I: contact model and application to cemented sand. *Comput Geotech* 75:192–209. <https://doi.org/10.1016/j.compgeo.2016.02.007>
- Itasca Particle Flow Code, PFC3D, ver 5.00, Itasca Consulting Group, Inc., 2014
- Iai S, Tobita T, Nakahara T (2005) Generalised scaling relations for dynamic centrifuge tests. *Geotechnique* 55(5):355–362. <https://doi.org/10.1680/geot.2005.55.5.355>

Publisher's Note Springer Nature remains neutral with regard to jurisdictional claims in published maps and institutional affiliations.